

# ADVANCED BLOWING MODEL FOR SOLID STATE TECHNOLOGY FUSES APPLIED TO SCHURTER'S COMPONENTS

Bruno Samaniego<sup>(1)</sup>, Laurent Trougnou<sup>(2)</sup>, Kaspar Gander<sup>(3)</sup>

*<sup>(1)</sup>Astrium  
31 rue des Cosmonautes - Z.I. du Palays  
31402 Toulouse Cedex 4 – France  
Email: bruno.samaniego@astrium.eads.net*

*<sup>(2)</sup>ESA  
Keplerlaan 1,  
2201 AZ Noordwijk, The Netherlands  
Email: laurent.trougnou@esa.int*

*<sup>(3)</sup>Schurter AG  
Werkhofstrasse 8-12  
CH-6002 Lucerne  
Email: kaspar.gander@schurter.ch*

## ABSTRACT

Whereas fuses based on wire technology can be modelled relatively easily applying Joule's first law on a single cylindrical wire in vacuum conditions, solid state fuses require much more complex modelling techniques in order to include the effects of several materials and a fuse element with a changing cross-section. As a matter of fact, solid state technology's main characteristic is that speed will not just depend on the fuse element but also on the surrounding items. This way, the choice of the adjacent materials and their shape is the key to determine both the speed and breaking capacity. Current space fuses can make use of up to seven different materials combined in a three-dimensional and not necessarily symmetrical design. These facts forbid drastic simplifications and limit the approaches used until now on wire fuse technology modelling.

Therefore, a new modelling methodology needs to be implemented in such way that a complex 3D fuse can be translated into a simple 2D model composed of equivalent electrical parts and available for use on any version of SPICE software. The reason to use such type of software is that an electrical macro-model of the fuse will allow performing system analysis in order to predict the fuse blowing effect at any point of the whole spacecraft power bus. This paper sets out the approach followed on the two different types of solid-state space fuses manufactured by Schurter: the MGA-S (rated current from 0.14A to 3.5A) and the HCSF (rated current from 7.5A to 15A) models. After a preliminary geometrical analysis, the fuse can be sliced into different sections of similar geometry. Each section will thus be reduced to a set of equivalent resistances by means of the shape factor method, and completed with capacitors resulting from an internal temperature distribution obtained thanks to a finite element method (FEM) analysis. The division of the original resistances and capacitors obtained in several ones will increase the accuracy of the fuse's speed determination as the time constant decreases.

The results have been compared to dedicated tests performed at Schurter's facilities, showing a very good correspondence with measured clearing time as a function of current (Time-current characteristics) and an encouraging potential to be used as a future fuse design tool.

## BACKGROUND

Telecommunication satellites can contain hundreds of fuses to protect payloads or equipments. Reliability and safety of the satellite often rely on these passive components. Consequently, a significant number of tests need to be performed in order to verify the compatibility of the fuse response to short-circuits and its impact on other equipments of the satellite (over-voltages, over-currents...). But tests can be very expensive if one needs to carry out hundreds of them, unless one can replace them by accurate and reliable electrical simulations.

Whereas fuses based on wire technology can be modelled relatively easily applying Joule's first law on a single cylindrical wire in vacuum conditions [1][2], solid state fuses require much more complex modelling techniques in order to include the effects of several materials and a fuse element with a non-uniform cross-section. As a matter of fact, solid state technology's main characteristic is that blowing time will not just depend on the fuse element but also on the surrounding items. This way, the choice of the adjacent materials and their shape is the key to determine both the

blowing time and breaking capacity. Current space fuses can make use of up to seven different materials combined in a three-dimensional and not necessarily symmetrical design. These facts forbid drastic simplifications and limit the approaches used until now on wire fuse technology modelling. Therefore, a new modelling methodology needs to be implemented in such way that a complex 3D fuse can be translated into a simple 2D model composed of equivalent electrical parts and available for use on any version of SPICE.

**OBJECTIVE: SPICE MODELS FOR REDUCING FUSE BLOWING TESTS AT SYSTEM LEVEL**

Why SPICE? The main reason to develop such models is to create a set of SPICE fuse components available for subsequent satellite electrical system simulation. Obviously, the theory presented hereafter could be applied on a specific fuse design tool since the principle can be perfectly valid, but this was not the original intention of the study. The final objective, as explained in the previous section, is to replace the fuse blowing tests at system level by accurate simulations, decreasing consequently the costs in terms of number of fuses, testbeds and time. It allows also avoiding stress on other equipments caused by over-voltages or over-currents.

The principle used on SPICE simulations is quite simple, and is described in Fig. 1. The current passing through the cold fuse will warm it up following Joule’s first law and the thermal model will derive the new temperature of the component. This variation will increase the fuse’s resistance and consequently the heat dissipated. If the current is big enough, the temperature will reach the melting point and the fuse will blow up.

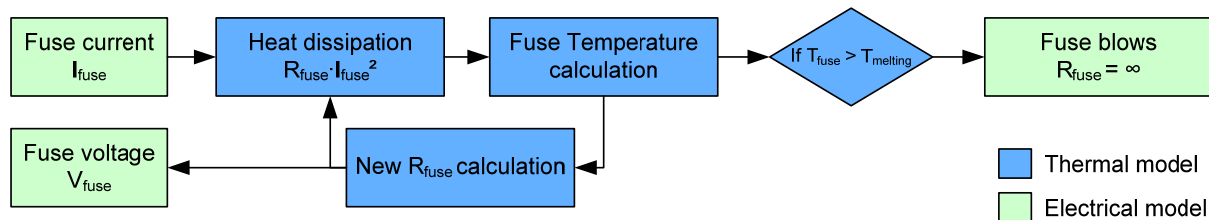


Fig. 1. SPICE simulation principle mixing thermal and electrical models

This principle has been translated into OrCAD Capture software in order to obtain a single component, with all the building blocks shown in Fig. 1, which can be easily implemented in a global electrical architecture. After presenting the principle and the implementation system, the thermal model can be analyzed and described in detail.

**MODELLING APPROACH FOR SOLID STATE TECHNOLOGY: MGA-S AND HCSF FUSES**

This paper sets out the approach followed on two different types of solid-state space fuses manufactured by Schurter: the MGA-S (rated current from 0.14A to 3.5A) and the HCSF (rated current from 7.5A to 15A) models.

Solid state technology does not use a wire fuse but a thick film technique. This fuse link, connected by two pads and surrounded by different layers and materials, makes the model more complex since the blow time will not just depend on the fuse element but also on the rest of the components. In addition, the geometry is far from a simple cylinder like the one presented in the Background section (see Fig. 2).

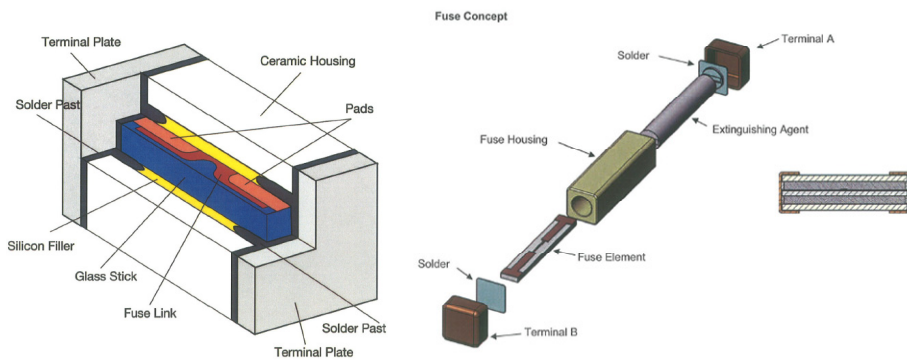


Fig. 2. MGA-S (left) and HCSF (right) fuses structural overview [3][4]

All along the study, several approaches have been examined in order to model in the most accurate way the heat dissipation and the blow-off sequence. The final approach will be the only one presented hereafter.

### MGA-S fuse geometry analysis

As it can be observed in Fig. 2, the structure of solid state fuses does not present any axis of symmetry that would allow an axial reduction into several concentric cylinders. In addition, the fuse does not have the same material composition lengthwise: following this direction, some sections contain the fuse element but not the pad elements and vice-versa, the fuse element geometry varies, etc. Consequently, the model will be “cut” into different slices depending on the composition and geometry. An example is presented beneath.

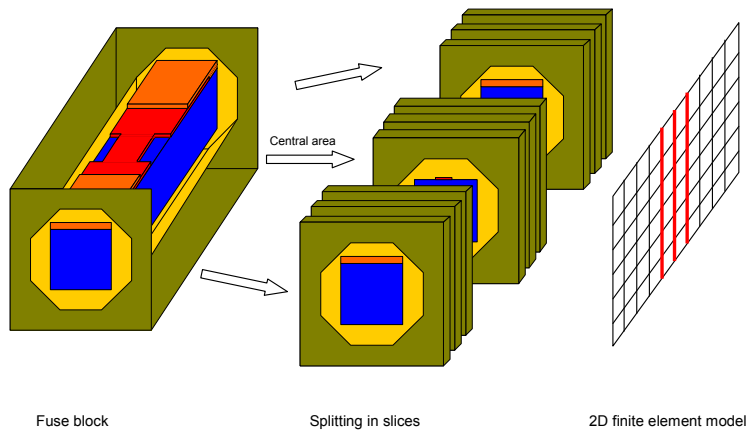


Fig. 3. 3D model to 2D model transition – MGA-S case

Afterwards, the slices are connected together through thermal resistances calculated following the same approach than the wire fuse [1]. Fig. 4 shows how the MGA-S has been sliced into seven different sections, depending on geometry variations. Since the fuse is mirror symmetric, sections 1, 2 and 3 are considered exactly the same on both ends of section 4.

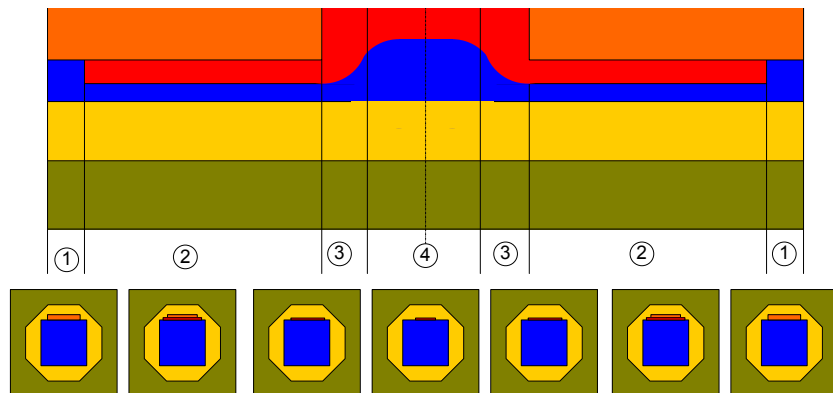


Fig. 4. Top view of the MGA-S fuse (left) and the different slices for each section (right)

Since geometry changes along the fuse element, it is logical to deduce that the electrical resistance will not be the same for every section. This will have a major impact on heat dissipation: section 4, for example, seems to be the section with less amount of fuse element and consequently more resistance. In order to quantify the real distribution, a simple integration of the different geometry profiles will give the distribution of the electrical resistance. These percentages will be multiplied by the cold resistance given by Schurter’s datasheet [3] (also called unsoldered resistance).

Table 1. Electrical resistance distribution for the MGA-S

Section	Resistance %
1	2.71%
2	13.97%
3	10.16%
4	46.33%
3	10.16%
2	13.97%
1	2.71%
<b>TOTAL</b>	<b>100.00%</b>

**Shape factors application: turning 3D models into 2D**

Fig. 5 shows the slice of the central section 4, where the red rectangle corresponds to the fuse link (aluminium), the blue square refers to the glass-stick, yellow represents the silicone filler and green part the ceramic housing [3]. Since the processing time required for determining very accurately the 2D heat distribution inside each slice would be prohibitive, some assumptions and simplifications need to be taken so the model will be accurate enough and much faster for a software like PSpice. A finite-element analysis (FEM) of the section is presented in Fig. 5. in steady-state, with the fuse link at 933 K (aluminium’s melting temperature) and the ceramic borders at 298 K (ambient temperature) in order to get an idea of the temperature distribution to be expected:

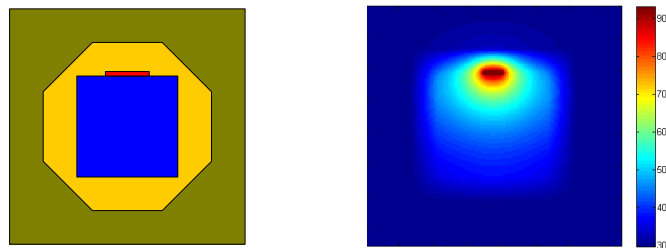


Fig. 5. Central section’s slice of the MGA-S fuse (left) and temperature distribution in K (right)

From this figure, it can be deduced that most of the heat transfer occurs between the fuse link and both the silicone and the glass-stick; on the contrary, the ceramic presents almost everywhere the same temperature. General conduction theory in heat transfer includes the shape factor approach for generic cases of 2D transmission. In fact, it allows the transition from a 2D geometry to a string of resistances that will include one parameter concerning the geometrical conditions: the shape factor  $S$  [5][6].

In this case, two shape factors could be applied, but first some important assumptions should be made:

- The fuse element (red) can be assumed to be a cylinder with the equivalent surface for heat exchange.
- Both the glass-stick (blue) and the silicone (yellow) can be mixed as a single material (with their conductivity and thermal capacity weighted) and be assumed to have a cylindrical shape.
- In the case of copper and aluminium, they will be coupled in parallel configuration, and the section will be assumed as circular with a mixed material following the same approach as the one used with the glass-stick..

Next figures detail the process of a new geometry assumption and shape factors calculation. If we assume the new configuration, the geometry of the ceramic will be:

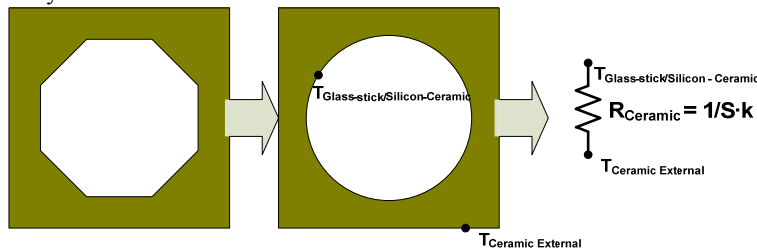


Fig. 6. Ceramic’s real geometry (left) and assumed one (right)

Assuming that the inner cylinder has a homogeneous temperature  $T_1$  (see Fig. 7), and that the external faces also have a homogeneous temperature  $T_2$ , the 2-D thermal distribution can be reduced to a single resistance

$$R = \frac{1}{S \cdot k} \tag{1}$$

Where,

- $S$  is the shape factor associated to the geometry, defined in this case in Fig. 7;
- $k$  is the thermal conductivity of the Ceramic.

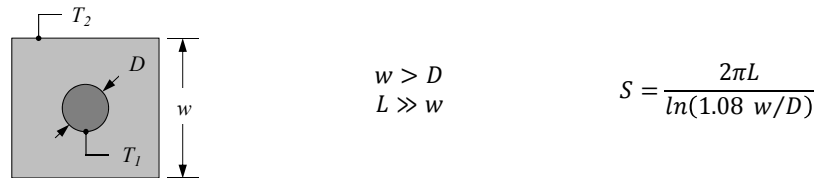


Fig. 7. Shape factor applied to an inner cylinder within a prism [6]

Once the ceramic is modelled, the inner cylinder composed of glass-stick, silicone and the fuse element can also be simplified:

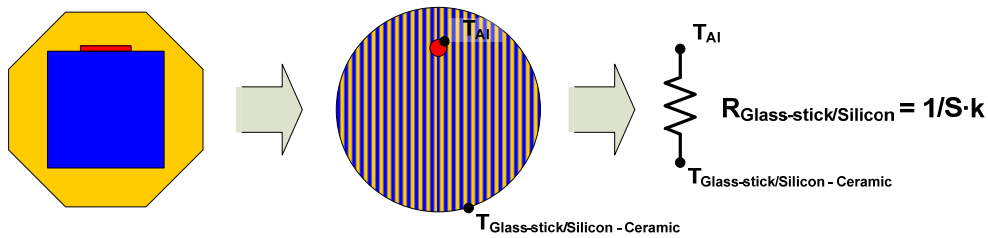


Fig. 8. Inner cylinder real configuration (left) and assumed one (right)

Assuming that the fuse element has a homogeneous temperature  $T_1$  (see Fig. 9), and that the external face of the glass-stick/silicone (remember that both materials have been mixed with their properties weighted [3]) also have a homogeneous temperature  $T_2$ , the 2-D thermal distribution can be reduced to a single resistance (see (1)) with a different shape factor:

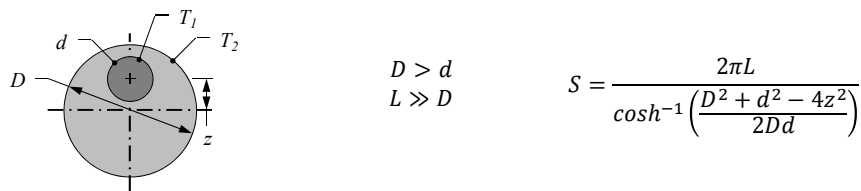


Fig. 9. Shape factor applied to a cylinder non-concentrically enclosed by a second cylinder [6]

Summarizing both shape factors, the global configuration will look as follows:

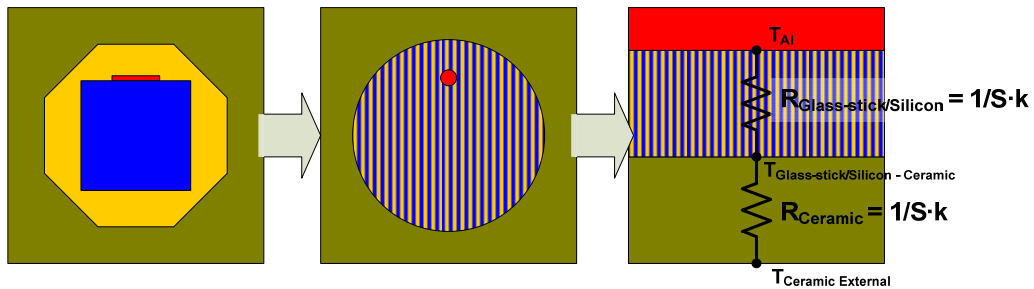


Fig. 10. Real section's slice of the MGA-S fuse (left), assumed new geometry (centre) and equivalent electrical scheme using the shape factors (right) for Section 4

The same process can be applied to each section of the fuse model. As already stated, each slice will be connected through 'horizontal' resistances calculated using the materials' physical parameters (thermal conductivity, area and length). For instance, the 'horizontal' resistance corresponding to the ceramic layer is:

$$R_{CeX} = \frac{L_X}{k_{Ce} \cdot A} \quad (2)$$

Where:

- $L_X$  is the horizontal length of the ceramic layer in mm;
- $A$  is the transversal area in  $\text{mm}^2$ ;
- $k_{Ce}$  is the ceramic thermal conductivity.

The global result for the MGA-S case is represented in the following figure:

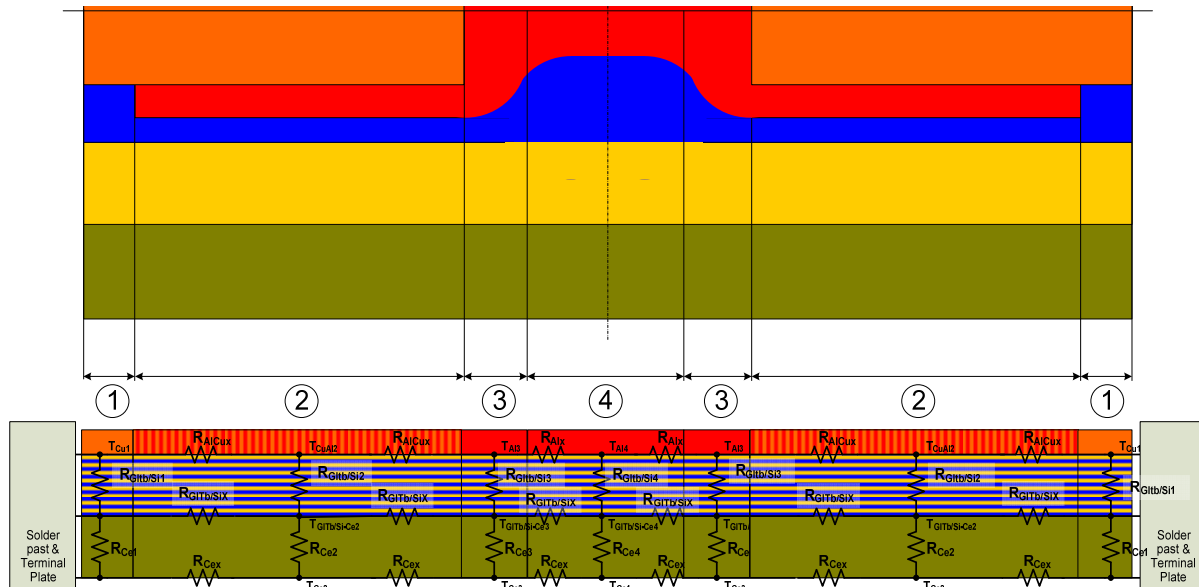


Fig. 11. Global result of the original geometry of the MGA-S fuse and the corresponding representation with thermal resistances

## Addition of thermal capacitances and their distribution

Until now, modelling of the solid state fuse technology has just included heat transfer in steady-state mode. Previous studies [1][2] have already explained how to include transient characteristics to a steady-state mode representation like the one shown in Fig. 11. Each thermal node, defined as black points in the previous figure surrounded by resistances and with a known (or computable) temperature, will contain an electrical capacity associated to the thermal capacity and the volume represented by the node. As an example, the thermal capacitances related to the thermal nodes of Section 4 are:

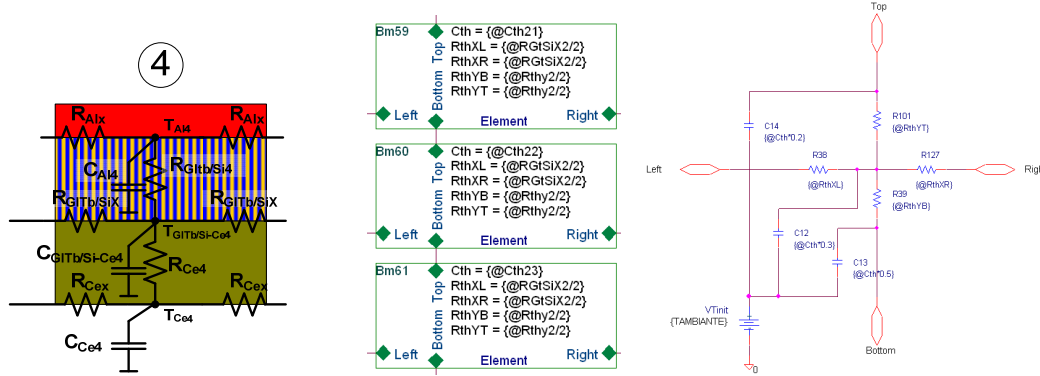


Fig. 12. Thermal capacitances corresponding to Section 4 (left), equivalent elements used for each layer in OrCAD Capture (centre) and detail of an element with the thermal node in the middle, thermal resistances and thermal capacitances (right)

The thermal capacitances are calculated as follows:

$$\begin{cases} C_{Al4} = C_{Al} \cdot V_{Al4} \cdot \rho_{Al} \\ C_{GITb/Si-Ce4} = C_{GITb} \cdot V_{GITb4} \cdot \rho_{GITb} + C_{Si} \cdot V_{Si4} \cdot \rho_{Si} \\ C_{Ce4} = C_{Ce} \cdot V_{Ce4} \cdot \rho_{Ce} \end{cases} \quad (3)$$

Where:

- $C$  is the Heat capacity of each material in [J/g.K]
- $V$  is the volume in [cm<sup>3</sup>]
- $\rho$  is the density in [g/cm<sup>3</sup>]

Once every node has its thermal capacitance associated, the model is finished. However, the temperature gradient for a single resistance like the one corresponding to the glass-stick/silicone can reach 550 K. This will lead to high resistance values and therefore time constants of few milliseconds or even seconds, which is unacceptable if we want to represent blow-off times in the range of 100 $\mu$ s.

The solution proposed in the frame of this project is to divide all thermal resistances and capacitances into several ones. For instance, the glass-stick/silicone layer is divided in 10 resistances in series (and consequently, 10 horizontal resistances in parallel) and the ceramic layer is divided in 4 resistances in series. Those numbers have been chosen in order to get enough accuracy and resolution in terms of time response (from 1ms of RC time constant for the higher short-circuit currents up to some seconds of time constant for the lower currents). The OrCAD Capture model will therefore be composed as shown in Fig. 13.

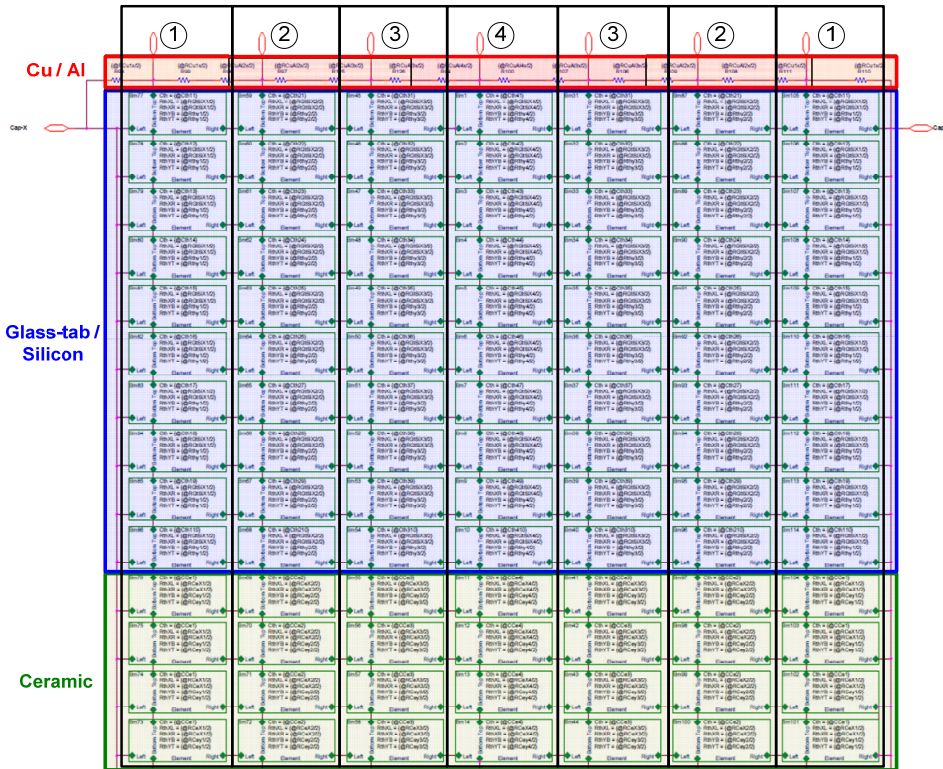


Fig. 13. OrCAD Capture complete thermal model with the various material layers shown in different colours

When it comes to multiple resistances in series, the first idea is to divide the initial resistance into 10 equal resistances. This way, one obtains ten equal temperature gradients and then the capacitors would be adapted according to the FEM analysis of the temperature distribution. An example will clarify this point.

The temperature distribution in steady-state mode of an MGA-S 1.4A is, in section 4:

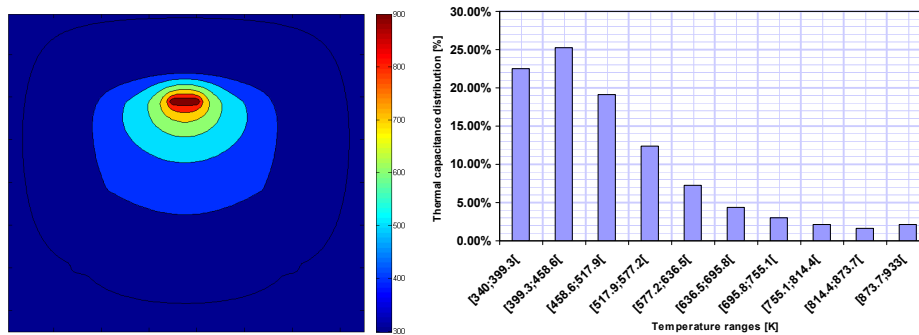


Fig. 14. Temperature distribution in steady-state mode of an MGA-S 1.4A - section 4 (left) and corresponding thermal capacitance distribution for the 10 Glass-stick/Silicon layers (right)

From the assumptions, we know that the external temperature of the aluminium is 933 K, from the FEM simulation, the temperature at the internal face of the ceramic is 300 K. There is consequently, a temperature gradient of 633 K in the glass-stick/silicone layer. If we divide the associated resistance into ten equal resistances, the gradient will be reduced to 63.3 K per resistance. The number of finite elements corresponding to the different intervals will tell us the percentage of thermal capacity for each layer. Lower temperatures get higher percentage since the model corresponds to a radial distribution, when the thermal capacitance increases with the radius. Each capacitance can then be calculated applying the percentage found here to the total thermal capacitance from (3).

## HCSF case

Fig. 2 gives the structure and composition of the HCSF fuse. It shows one plane of symmetry that can be used in order to get a simplified model; as for the MGA-S case, different materials are used to surround the fuse element (copper this time), but in this case the base-material is different from the glass-stick previously shown. The base-material and the silicone, having closer physical properties [4] will be considered as one with weighted properties. Again, each copper section will be considered as one single cylinder with the corresponding heat-exchange surface.

The transversal section in the central part of the fuse and the corresponding approach through shape factors [5] are:

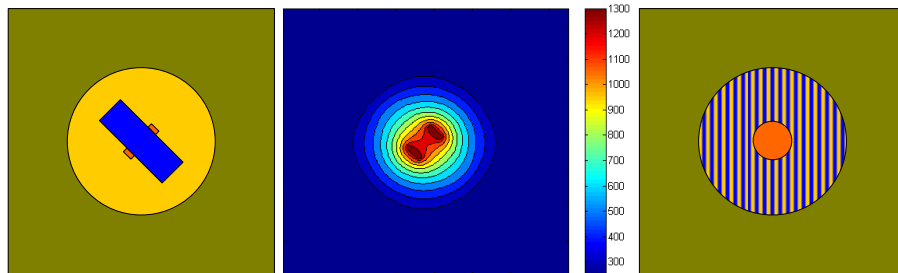


Fig. 15. Real section 4 of the HCSF fuse (left), simulated FEM analysis (centre) and assumed new geometry (right)

The left figure shows the cross-section at the centre part of the HCSF fuse: the orange areas correspond to the copper fuse element, the base-material is represented by the blue rectangle and the silicone is the yellow part. Green surrounding area refers to the ceramic fuse housing.

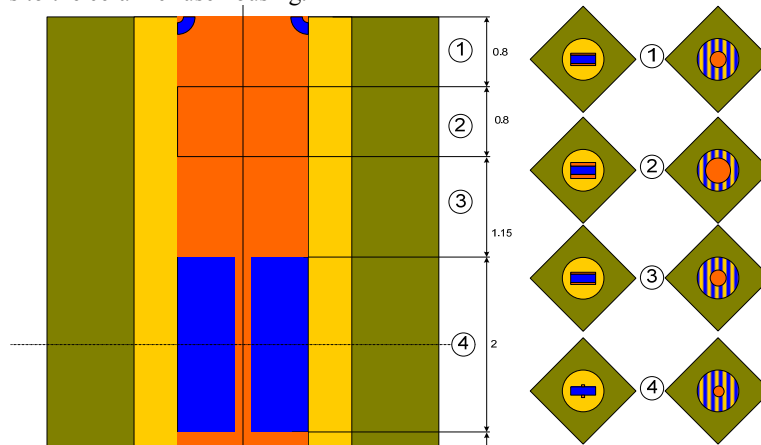


Fig. 16. HCSF top view, sections chosen and corresponding geometry adaptations

A FEM analysis (see Fig. 15) concerning the thermal conduction in steady-state shows how the temperature distribution around the copper areas quickly becomes a radial distribution and can be replaced by a much simpler geometry.

This method can be applied to the rest of the HCSF fuse, decomposed in several sections, just like the MGA-S case. In fact, the same OrCAD Capture model can be utilized. The user just needs to modify the thermal parameters; the value of the electrical resistance and its distribution among the sections like presented in Table 1, the structure of the model can be kept as is.

## ARCING MODEL

Up to now, when the fuse element reached the melting temperature, the fuses' resistance instantaneously increased from some  $m\Omega$  up to  $1G\Omega$ , but this is not how the fuse behaves in reality. After all the tests performed at Schurter's facilities, several approaches have been studied in order to find an equation representing the evolution of the resistance with time (exponential, polynomial...). Finally, it has been observed on many test cases that voltage and current were varying almost linearly (see Fig. 17), resulting in a particular resistance evolution profile that could be common to every model (see Fig. 19).

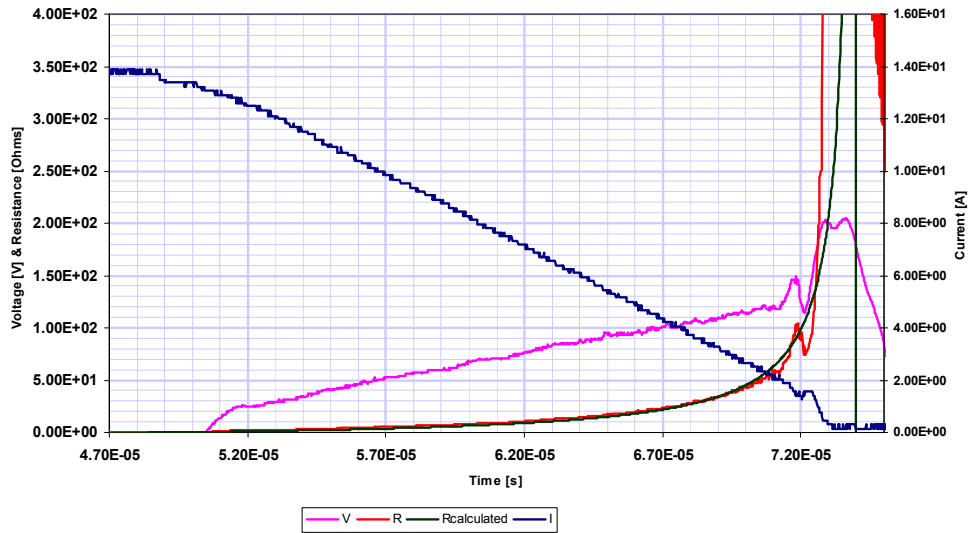


Fig. 17. Arcing test result on MGA-S 1.4A at 1000% with the real resistance evolution (red) and the one from the model (dark green)

In order to model the arcing response, the resistance will evolve with time, starting when the melting temperature is reached. The theoretical approach has been to assume that voltage and current evolve both linearly with the following profiles:

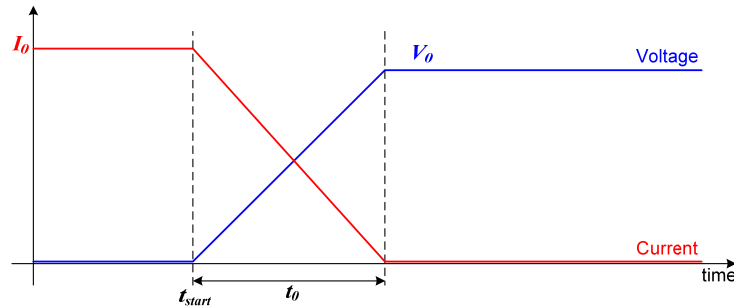


Fig. 18. Theoretical evolution of current and voltage during the arcing phase

First, current and voltage are expressed as equations:

$$\begin{cases} I = I_0 \left( 1 - \frac{t - t_{start}}{t_0} \right) \\ V = V_0 \left( \frac{t - t_{start}}{t_0} \right) \end{cases} \quad (4)$$

Where:

- $I_0$  is the initial current;
- $V_0$  is the final voltage;
- $t_{start}$  is the time when the melting temperature is reached;
- $t_0$  is the duration of the arc.

With these profiles, the resistance can be easily determined (with  $R_0 = V_0/I_0$ ):

$$R = R_0 \frac{\left( \frac{t - t_{start}}{t_0} \right)}{\left( 1 - \frac{t - t_{start}}{t_0} \right)} \quad (5)$$

The different values for the parameters will be established for the different fuse models. It has been observed that for different current rates, the resistance profiles are very similar. This fact will simplify the number of models and it will be assumed that all MGA-S fuses have the same arcing profile and so do the HCSF.

In the case of the HCSF model, the parameters ( $R_0, t_0$ ) to be applied change from the ones used on the MGA-S and give the following results:

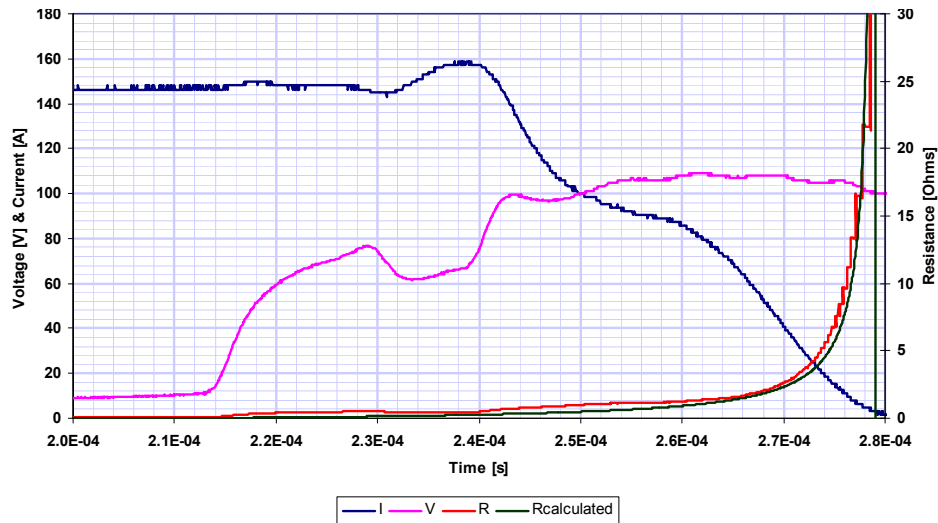


Fig. 19. Arcing test result on HCSF 15A at 1000% with the real resistance evolution (red) and the one from the model (dark green)

The time-dependent resistance is then implemented in OrCAD Capture thanks to Analog Behavioral Modeling (ABM) with the results shown in the coming sections.

## TEST CORRELATION RESULTS

Even if all the different Schurter's fuses have been modelled and many rated currents have been tested, only two models will be presented in this paper for practical reasons.

The model MGA-S 1.4A was tested and can therefore allow a more detailed comparison rather than just the datasheet's specifications. As it can be observed in Fig. 20 (left), the model is absolutely within the limits established by the datasheet and really close to the test results. It has to be noticed that, when there is no model result, it means that the fuse did not blow off. Usually, when small currents go through the fuse, the model loses much accuracy. In this case, the mean time error was 25.6%, with a minimum error of 12.8% (corresponding to the 600% of  $I_R$  case).

The model HCSF 7.5A was one of the HCSF fuses tested and used for the blowing time correlation. The result is summarized in Fig. 20 (right). In this case, all the rated currents that made the fuses blow during the tests made it also during the simulations. The curve corresponding to the simulated case, always under the test curve, represents a worst case for the blowing time. The mean time error is 44.4%, with a minimum value at 400% of the rated current: 27.4%.

It needs to be highlighted that these results give good correlations for the short blowing times, which are of primer interest for the system simulations. The model's curve remains always within the limits established in Schurter's datasheets [3][4]. By tuning some parameters like the unsoldered resistance (coming directly from test measurements and always within the range values provided by the manufacturer for example), or the distribution of thermal capacitance, the curve can be adjusted to a precise set of data, like the tests results.

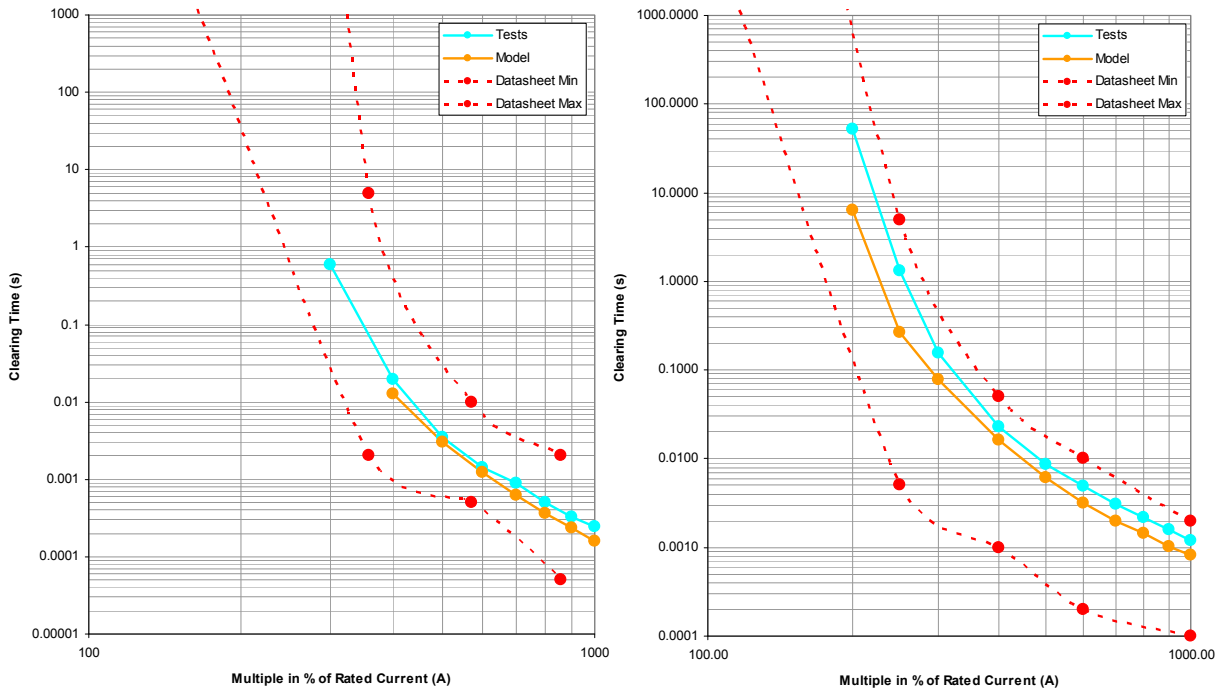


Fig. 20. Blow time curve for MGA-S 1.4A (left) and HCSF 7.5A (right)

### SATELLITE POWER BUS SETUP AND ASSOCIATED TESTS

Once the fuse has been completely modelled and the model validated for every current range tested, it is time to verify the final objective of the study: to validate the behaviour of a complete satellite electrical system and check the effects of a short-circuit, the resulting fuse blow-off and every over-current or over-voltage anywhere in the system.

The electrical architecture of a telecommunications satellite from the Astrium's EUROSTAR 3000 platform has been taken and simplified for this purpose. Fig. 21 shows the whole architecture: a Power Supply Regulator (PSR) reduced to a single capacitor with a capacitance around 2 mF. From the PSR, two Power Distribution Units (PDU) are powered up and three Equipments Under Test (EUT) represent the equipments to be short-circuited.

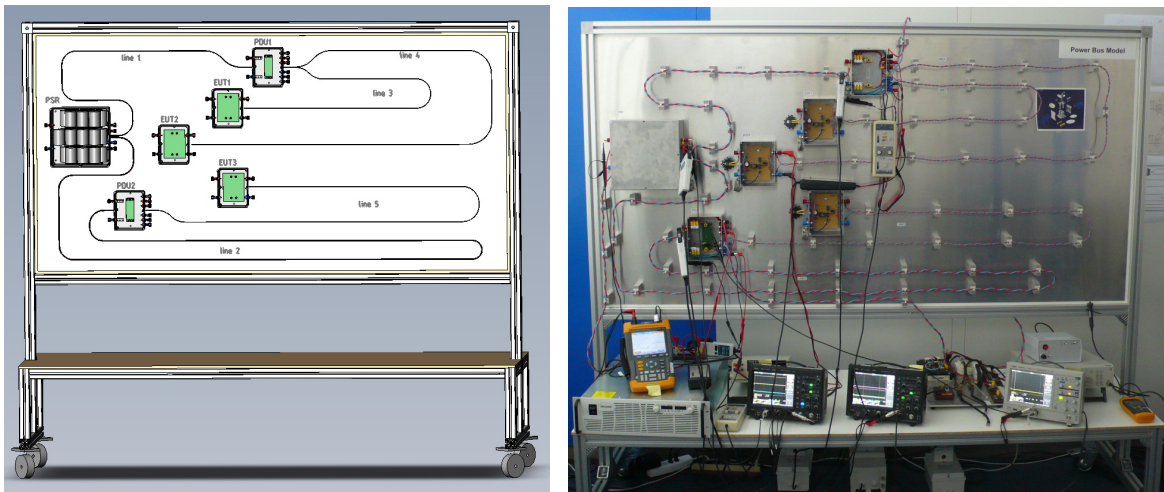


Fig. 21. Sketch-up of the test set-up (left) and picture of the real one at Schurter's facilities (right) -Source: Schurter AG

Again, just one case will be presented in this paper: the MGA-S 2.1A for instance. This will be the opportunity to verify the results of the model as it was created from the original geometry and how it can be tuned for better results and further use. The figures presented hereafter show the results after identification of the key parameters of the fuse model and its modification thanks to the tests results. For instance, it can be appreciated how, by changing the unsoldered resistance from 28 mΩ to 23 mΩ, the blow time matches almost perfectly.

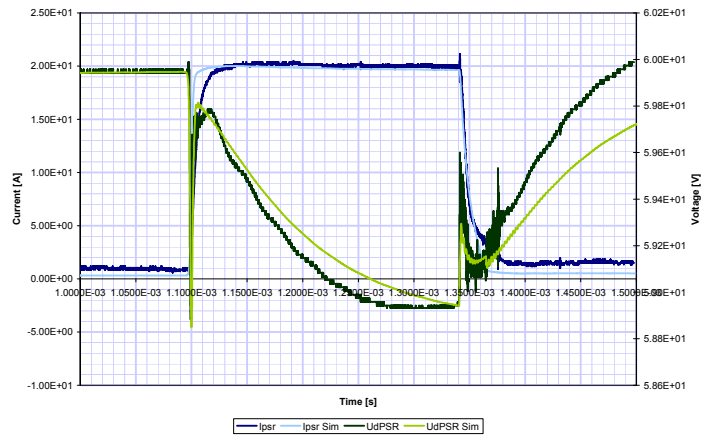


Fig. 22. PSR current and differential voltage at PSR's output with tuned parameters

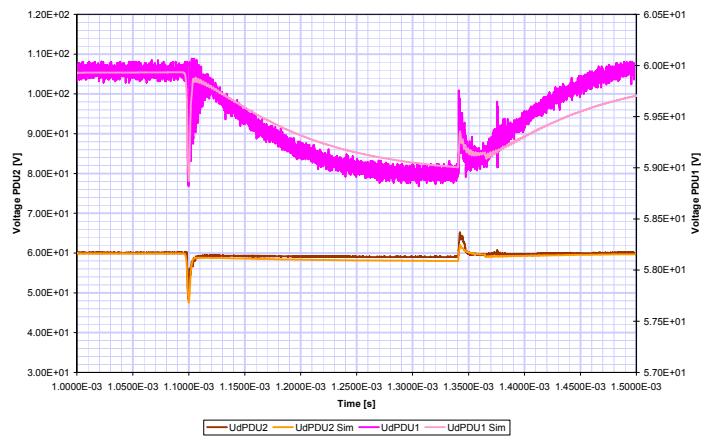


Fig. 23. Differential voltages at PDU1 and PDU2 outputs with tuned parameters

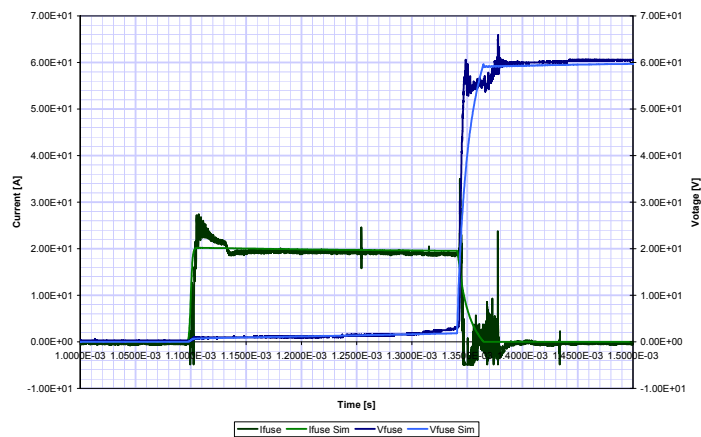


Fig. 24. Fuse current and voltage with tuned parameters

Finally, it can be observed that over-voltages and over-currents do appear when a short-circuit occurs and also when the fuse latches-up. The results of the correlation show that transient effects can be reproduced with high accuracy and be used in the future as representative and complementary information for tests validation or even substitution.

## **CONCLUSION**

It has been demonstrated that Solid State technology fuses can as well be modelled as the Wire technology for further integration in more complex electrical systems. Even if many more calculation steps and accurate information are required to have a fuse model as representative as the ones presented in [1] and [2], the shape factor method is definitely the best suited for this kind of simulations.

During the study, many lessons were learnt and many clues were imagined for up-coming model improvements. The FEM analysis is not accurate enough and would require more powerful software to obtain a better distribution of thermal capacitance. The number of thermal nodes could also be increased, always being careful not to make the model too complex thus slowing down the simulation. Finally and most importantly, the more we know about fuse geometry and composition, the more accurate the model will be. This means that the model needs to follow any minor change on the design and each rated current should be modelled independently for an optimal performance when it is integrated into a global electrical system.

## **REFERENCES**

- [1] Astrium, "Reducing EMC verification for future Telecom PF", Contract 18722/05/NL/AG, 2005-2007.
- [2] Astrium, "Modelling and numerical simulation of fuse behaviour (thin nickel or silver wires)", Contract 98/P2/NL/LC.
- [3] Schurter, "MGA-S (SMD-Fuse for Space applications datasheet)", Ref. 0105.1950, 2005.
- [4] Schurter, "HCSF datasheet", Ref. 0105.2099, 2010.
- [5] J.E. Sunderland and K.R. Johnson, "Shape factors for heat conduction through bodies with isothermal or convective boundary conditions", ASHRAE 71st Annual Meeting in Cleveland, Ohio, 1964.
- [6] F.P. Incropera and D.P. Dewitt; "Introduction to Heat Transfer"; Prentice Hall; Mexico 1999.